Electric field dependence of positronium formation in condensed matter*

Werner Brandt and Jason Wilkenfeld†
Department of Physics, New York University, New York, New York 10003
(Received 16 December 1974)

Electrostatic fields affect the lifetime spectra of positrons annihilating in normal paraffins and polyethylenes. The intensity of the longest lived of the three resolved lifetime components decreases by almost 50% at the highest fields (~200 kV/cm). The dependences of the data on density, temperature, and electric field are interlinked in a comprehensive manner by a theory which depends parametrically on the cross sections for the interaction of epithermal positrons with the molecular ($-CH_2-$) repeat units. Inferences are drawn for electronic subionization processes in insulators.

I. INTRODUCTION

In previous papers of this series, henceforth referred to as I–V, [1–4] experimental and theoretical studies of the positron annihilation in condensed molecular substances were reported from a unifying point of view. [5] The present paper VI reports data on the effect of applied electrostatic fields on the positron lifetime spectra in a homologous series of condensed paraffins of molecular structure $CH_3(-CH_2-)_{n-2}CH_3$, where $n=5$, 6, 9, 14, 17, 20, and "∞" (polyethylene). Based on the theory given in III, the electric field effect permits estimates of cross sections for the interaction of epithermal positrons with molecules in condensed matter.

Electric fields are known to enhance Ps formation in simple gases[6–8] and liquid He[9] by accelerating slow positrons into the Ore gap, i.e., the range of kinetic positron energies near the ionization threshold of the molecules where positronium (Ps) formation is most probable. In the gas SF_6, a marked decline at low fields precedes the rise above the zero-field Ps yield at high fields. [7,8] In the molecular solids polyethylene $(-CH_2-CH_2-)_n$ and polytetrafluoroethylene $(-CF_2-CF_2-)_n$, only a decrease has been observed due to fields as high as 250 kV/cm. [10,11] No field effect has been found in dipolar solids such as poly (methylmethacrylate) (PMMA) and nylon. [10]

The paraffins were selected for this study because exploratory measurements showed large field effects in polyethylene, [11] and because Crow, Sharbaugh, and Bragg[12] found that the electric breakdown strength of linear paraffins decreases with increasing free volume between the molecules. Since subionization scattering of positrons and electrons on molecules are similar, [13] the field-dependent Ps yield should also be a function predominantly of the free volume. Our results support this contention. They suggest a change in the assignments of the three resolved lifetime components given in II.

II. EXPERIMENTAL

A. Apparatus

Positron lifetime spectra were measured with a conventional fast-slow delayed coincidence apparatus[14] with prompt resolution set at 350 psec and a decay slope of 1×10^{-2} psec^{-1}. Sources of ^{22}Na in envelopes of 6-μm Al foil were sandwiched between 0.2-g/cm^2 samples, which stopped all positrons, and the package was clamped between grounded electrodes. The source envelope served as the high-voltage electrode. The applied field at voltage settings of ≤ 10 kV was known to 5% and stable to 0.25%, and above 10 kV to 10% and 0.5%, respectively.

Each lifetime measurement was performed at least twice, viz., with the source electrode once positive and once negative with regard to ground. No polarization effects were found, in agreement with theoretical estimates[15] that internal screening of the fields in these substances is negligible. Therefore, the internal field is set equal to the applied field. We found no evidence of the polarization effects reported by Stevens and Lichtenberger. [16]

The spectra were resolved by a modified Cumming program[17] and the FITME program[18] into three components. The lifetime information is thus contained in six spectral parameters, the normalized intensities I_A, I_B, and I_C, where $I_A+I_B+I_{C'}=1$, and the respective lifetimes $\tau_A>\tau_B>\tau_{C'}$ or disappearance rates $\gamma_A\equiv\tau_A^{-1}$, $\gamma_B\equiv\tau_B^{-1}$, and $\gamma_{C'}\equiv\tau_{C'}^{-1}$.

B. Materials

Samples were prepared from linear (normal, n-) paraffins, with the structure $H_3C-(-CH_2-)_{n-2}-CH_3$, for $n=5$, 6, 9, 14, 17, 20 and "∞" (polyethylenes). At the temperature of the experiment (22 °C), the materials $n\leq17$ are liquids. They were obtained from Phillips Petroleum (99% mol pure). Eicosane ($n=20$) came from Eastman Kodak and K+K Labs

(97% mol pure, no measureable difference). Five polyethylenes were prepared with different crystallinities ranging in density from 0.917 to 0.967 g/cm^3.[19] Measurements were also made on poly (methylmethacrylate) (PMMA; Rohm-and-Haas, commercial grade), polytetrafluoroethylene (TFE; DuPont, 60% volume crystallinity) and on fluorinated ethylene-propylene copolymer (FEP; DuPont, 50% volume crystallinity).[19] Properties[19,20] are listed in Table I.

The paraffins were filtered through glass fritters and degassed by standard freeze-thaw techniques to remove oxygen. The presence of oxygen reduces the mobility of certain impurities by complex formation,[21] which increases the breakdown strength. We chose to remove oxygen to obtain unquenched lifetime spectra, which limited the maximum fields to some 250 kV/cm without incurring electric fatigue followed by breakdown.

III. RESULTS

A. Zero field

The intensities and lifetimes are listed in Table I. The data for FEP, TFE, and PMMA agree with previous measurements.[2,22] Figure 1 shows τ_A as a function of $V^* = (V_0 d)^{-1}$, where d is the density listed in Table I. The excluded specific volume V_0 is calculated from the relation $V_0 = \pi/2\sqrt{3} \times d(T \to 0\ ^\circ\mathrm{K})$ given in I, with the result $V_0 = 0.84$ cm^3/g. Included are data by Wilson, Johnson, and Stump[23] on polyethylene at 30 °C in the pressure range 1–10^4 atm; the temperature data from II; the data at 22 °C by Gray, Cook, and Sturm[24] for n-paraffins $n = 4, 5, \ldots 18$; n-octane data by Buchikhin, Goldanskii, and Shantarovich[25] between −15 and 115 °C; and the temperature data between 25 and 175 °C by Thosar, Kulkarni, Lagu, and Chandra.[26]

The curves are predictions of the pickoff lifetime τ_P, which we identify with τ_A. In I, II, and V, it was shown in terms of a simple cell model that τ_P depends on V^* and the reduced temperature $T^* = T/\Theta_D$ ($\Theta_D = 123$ °K, Debye temperature[27]) as

$$\tau_P = \tau_0 \frac{1 + F(S, V^*)}{1 + G(S, V^*)(e^{H(S, V^*, T^*)} - 1)} , \tag{1}$$

where τ_0 is the pickoff lifetime at $V^* = 1$ and $T^* = 0$. The strength parameter $S = (4m/\hbar^2) U_0 r_0^2$ of the molecular potential U_0 of radius r_0 in paraffins is $\simeq 60$. In these materials, the function H can be approximated by

$$H = \begin{cases} 0, & T^* < 1 \\ 2\xi^2 V^* \gamma_M (T^* - 1)/(T_M^* - 1), & 1 < T^* < T_M^* \\ 2\xi^2 V^* \gamma_M , & T_M^* < T^* . \end{cases} \tag{2}$$

The melting point T_M appears as $T_M^* = T_M/\Theta_D$. In V, the functions F, G, and ξ are tabulated and approximate analytical forms given.

The constant γ_M is proportional to the mean-square amplitude of thermal vibrations at T_M of a statistical molecular segment length of mass M_{eff}, and related to the effective phonon mass $M_{\mathrm{ph}}(T_M) = k_B T_M/s^2$ (s = velocity of sound) as

$$\gamma_M = M_{\mathrm{ph}}(T_M)/M_{\mathrm{eff}} . \tag{3}$$

We find that for normal paraffins, $M_{\mathrm{ph}}(T_M) \simeq 1.22 \pm 0.05$ amu. The statistics of chain molecules suggests that

$$M_{\mathrm{eff}}(n) = M_{\mathrm{CH_2}}\, n_0 (1 - e^{-n/n_0}) , \tag{4}$$

where $M_{\mathrm{CH_2}} = 14$ amu and n_0 is the mean number of CH_2 groups in a statistical segment. Figure 2 compares values of γ_M^{-1} as determined from the τ_A data in Table I and in Ref. 24 with Eqs. (3) and (4), giving $n_0 \sim 5$ for $n > 8$ and a constant $\gamma_M \simeq 9 \times 10^{-3}$ for $n \leq 8$. That is, the persistence length for correlated thermal motion of long condensed paraffin molecules is comparable to the intermolecular distances.

Figure 1 shows five curves calculated with $S = 60$: (1) the rise of τ_P predicted for $T^* \ll 1$; (2) the isobaric rise with T^* without melting, and (3) with the melting included for polyethylene (cf. arrow on abscissa) which agrees with the data. The curve 5 is calculated for $n = 8$ and follows closely the data for n-octane. The remaining isothermal (room temperature $T^* = 2.4$) data on liquids demonstrate how n influences V^* (as labeled on the inserted n scale) and, through V^* and γ_M, the pickoff time: through each point measured for a liquid with a given n passes a rising curve similar to curves 3, 4, and 5, which predicts the behavior if $V^*(T)$ of the sample is changed by temperature or pressure. One concludes that the model leading to Eq. (1) can account in detail for the volume and temperature dependence of all τ_A data on paraffins. The relation to the angular correlation is discussed in an appendix.

Figure 3 compares the I_A values from Table I with the formula derived in II,

$$I_A = \tfrac{3}{4} \Phi_0 \exp[-V_{\mathrm{cr}}^*/(V^* - 1)], \tag{5}$$

where Φ_0 is the total Ps yield and $V_{\mathrm{cr}}^* = 0.23$ is the minimum free volume necessary for Ps formation. Equation (5) accounts for the large I_A difference between the isomeric compounds n-pentane ($I_A = 0.35$) and 2, 2-dimethylpropane ($I_A = 0.44$).[24]

The electric field effect presented in Sec. IV combined with the data discussed here suggest the following assignments of the three lifetime components. They differ from those given in II.[28]

(a) The intensity of the longest-lived component, I_A, comprises all o-Ps formed, as implied by Eq. (5).

TABLE I. Summary of positron lifetime data.

Substance	$d_{20/4}$ (g/cm^3)	V^*	T_M (°K)	Zero-field components[f] I_A	τ_A (nsec)	I_B	τ_B (nsec)	$I_{C'}$	$\tau_{C'}$ (nsec)	Field dependence of I_A $(dI_A/d\mathcal{E})_{\mathcal{E}\to 0}$ (cm/MV)	$\mathcal{E}_{max}$ (kV/cm)	$I_A(\mathcal{E}_{max})$
n-alkanes $[CH_3(CH_2)_{n-2}CH_3]$												
Pentane $n=5$	0.626[a]	1.901[e]	143[a]	0.37	4.35	0.18	0.68	0.45	0.28	3.0	65	0.29
Hexane $n=6$	0.660	1.803	178	0.37	3.99	0.21	0.59	0.42	0.26	3.0	60	0.27
Nonane $n=9$	0.718	1.658	222	0.36	3.52	0.24	0.47	0.40	0.23	2.6	50	0.27
Tetradecane $n=14$	0.763	1.560	267	0.33	3.38	0.11	0.78	0.56	0.31	3.2	95	0.25(∞)[h]
Heptadecane $n=17$	0.778	1.530	295	0.33	3.27	0.15	0.64	0.52	0.29	3.2	65	0.26
Eicosane $n=20$												
Liquid	0.766[b]	1.553	310	0.33	3.30	0.15	0.63	0.52	0.27	c	c	c
Solid	0.909	1.309	310	0.23	1.26	g	g	0.75	0.30	1.8	15	0.20
Polyethylenes $(-CH_2-CH_2-)_n$												
A15 (46%)[d]	0.917	1.298	~385	0.27	2.61	0.10	0.65	0.63	0.31	1.6	250	0.14(∞)
CS (51%)	0.925	1.290	~385	0.24	2.67	0.09	0.81	0.67	0.33	1.3	225	0.12
P106 (53%)	0.930	1.280	~385	0.22	2.54	0.09	0.87	0.69	0.31	1.1	150	0.15
P111 (69%)	0.948	1.255	~395	0.18	2.53	0.10	0.80	0.72	0.32	0.8	150	0.14
A7516 (80%)	0.967	1.231	~395	0.18	2.54	0.09	0.75	0.73	0.34	1.0	250	0.11(∞)
Fluorocarbons $(-CF_2-CF_2-)_n$												
Teflon TFE (60%)[d]	2.17		<600[i]	0.16	4.17	0.18	1.02	0.66	0.31	0.3	185	0.13
Teflon FEP (50%)	2.14		<563[i]	0.20	3.75	0.08	0.92	0.72	0.32	0.0	175	0.19(∞)
Poly(methylmethacrylate) $[-CH_2C(CH_3)(COOCH_3)-]_n$	1.19		j	0.27	1.94	0.11	0.62	0.62	0.33	0.0	225	0.26(∞)

[a]Densities and melting points for $n \leq 17$ are taken from the *Handbook of Chemistry and Physics*, 29th ed. (Chemical Rubber, Cleveland, 1968).

[b]At 55°C for the liquid and 20°C for the solid, W. E. Seyer, R. F. Patterson, and J. L. Keays, J. Amer. Chem. Soc. 66, 179 (1944).

[c]No field-dependent data were obtained. It is conjectured that the trend in intensities under an applied electrostatic field is similar to that for *n*-tetradecane, for example, of comparable density.

[d]Percentages in parentheses are fractional volume crystallinities furnished with densities by J. M. Watkins, Jr. (private communication).

[e]Reduced specific volume, $V^* = 1/V_0 d$ where $V_0 = 0.84$ cm^3/g for paraffins as calculated according to W. Brandt, S. Berko, and W. W. Walker [Phys. Rev. 120, 1289 (1960)].

[f]Averages of two to four runs are given. The component intensities are reproducible to 5% in I_A, 20% in I_B, and 5% in $I_{C'}$; the lifetimes are reproducible to 1% in τ_A, 20% in τ_B, and 10% in $\tau_{C'}$.

[g]A component corresponding to I_B in the other compounds is included in $I_{C'}$ here. An additional component was resolved of intensity ~0.03 with a lifetime > 3 nsec.

[h]A value of $I_A(\mathcal{E}_{max})$ followed by (∞) is judged to represent the asymptotic limit at high fields.

[i]The melting point is that for samples of 100% crystallinity. Partially amorphous samples soften at lower temperatures.

[j]Amorphous completely, no well-defined melting point.

(b) The intensity of the intermediate lifetime component, I_B, comprises positrons which have been localized in disordered regions with pockets of free volume larger than some value V_t^*, to form A^+ centers[29] with probability β_0. Then

$$I_B = (1 - \tfrac{4}{3} I_A)\beta_0 \exp[-V_t^*/(V^* - 1)]. \quad (6)$$

(c) The intensity of the resolved shortest-lived component is

$$I_{C'} = \tfrac{1}{3} I_A + (1 - \tfrac{4}{3} I_A)(1 - \beta_0) \exp[-V_t^*/(V^* - 1)]. \quad (7)$$

The prime on the subscript indicates that it refers to a composite lifetime component, consisting of the p-Ps pendant of o-Ps and the positrons annihilating in the bulk.

Comparison of Eq. (6) with the data in Table I (solid curve B in Fig. 3) gives $\beta_0 = 0.62 \pm 0.06$ and $V_t^* = 0.4$. The latter value is comparable to that of the mean free volume in amorphous polyethylene.

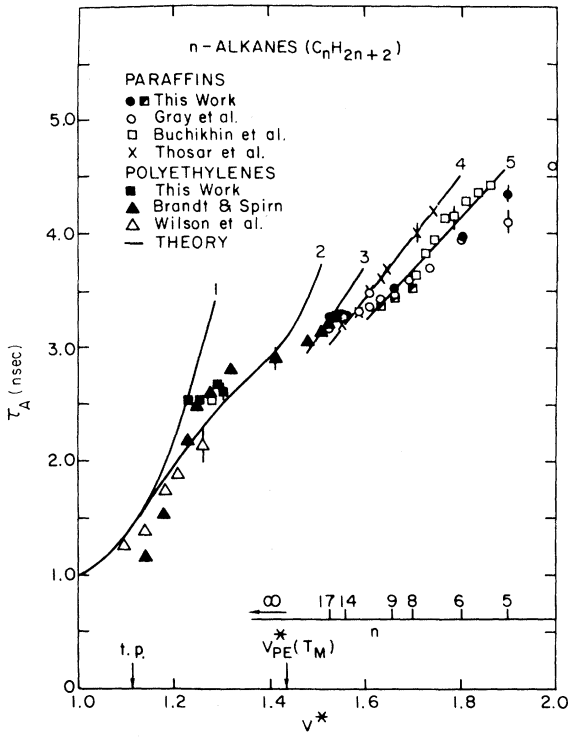

FIG. 1. Long lifetime for the homologous series of paraffins and polyethylenes listed in Table I as a function of reduced specific volume $V^* = (V_0 d)^{-1}$, where $V_0 = 0.84$ cm^3/g is the specific volume of the excluded molecular core. Tight packing for the long-chain cylindrical molecules occurs at $V^*_{t.p.}$. The reduced specific volumes at 20 °C and 1 atm are shown for pentane ($n = 5$), hexane ($n = 6$), octane ($n = 8$), nonane ($n = 9$), tetradecane ($n = 14$), and heptadecane ($n = 17$). Points to the left of $V^*_{PE}(T_M)$, the reduced specific volume of polyethylene (PE) ($n = \infty$) at its approximate melting point. The curves represent Eq. (1) and are discussed in the text.

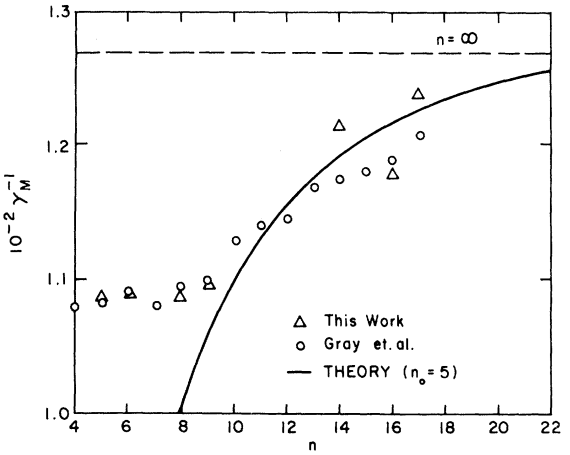

FIG. 2. Values, deduced from measured lifetimes, of the reciprocal of the mean-squared amplitude γ_M, of the intermolecular vibrations at T_M, in units of the mean-square radius of the molecular cell vs n. The curve represents Eqs. (3) and (4).

B. Electric field dependence

The three lifetimes in all substances investigated (Table I) remain constant, within experimental uncertainties, under the influence of elec-

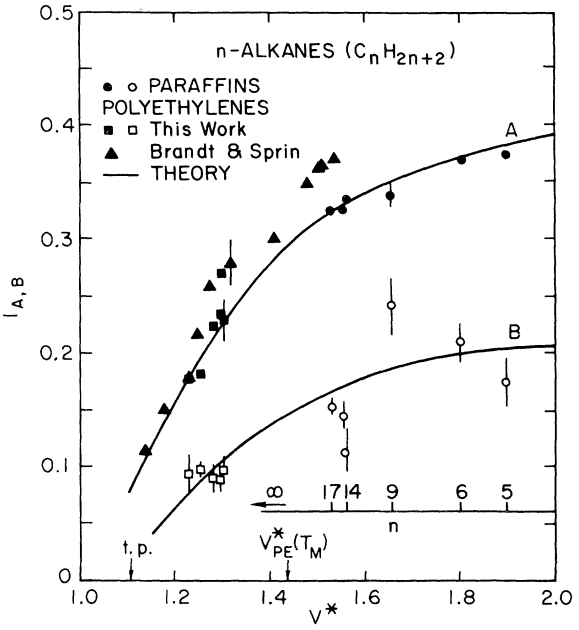

FIG. 3. Relative intensities of components A and B for the paraffins and polyethylenes listed in Table I plotted as a function of the reduced specific volume. The curves represent Eqs. (5) and (6).

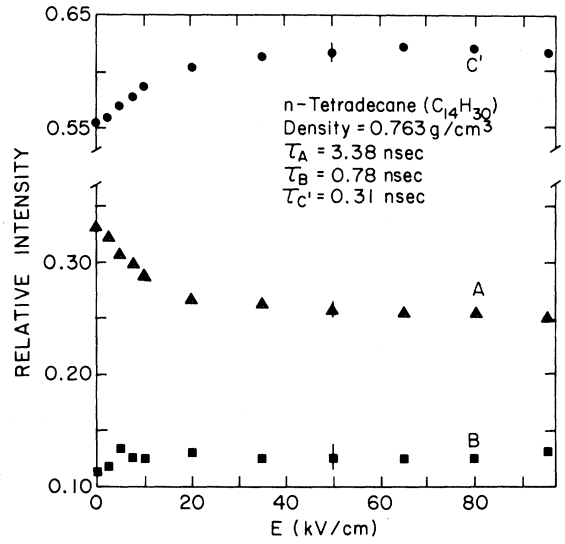

FIG. 4. Relative intensities of the three resolved components in the positron lifetime spectra of *n*-tetradecane [$CH_3-(CH_2)_{12}-CH_3$] vs the applied field. Representative error bars are shown for each component.

tric fields $\mathcal{E}$ up to 250 kV/cm. The intensities of the paraffin spectra vary significantly. Examples are shown in Figs. 4 and 5.

In the paraffins, $I_A(\mathcal{E})$ decreases linearly at

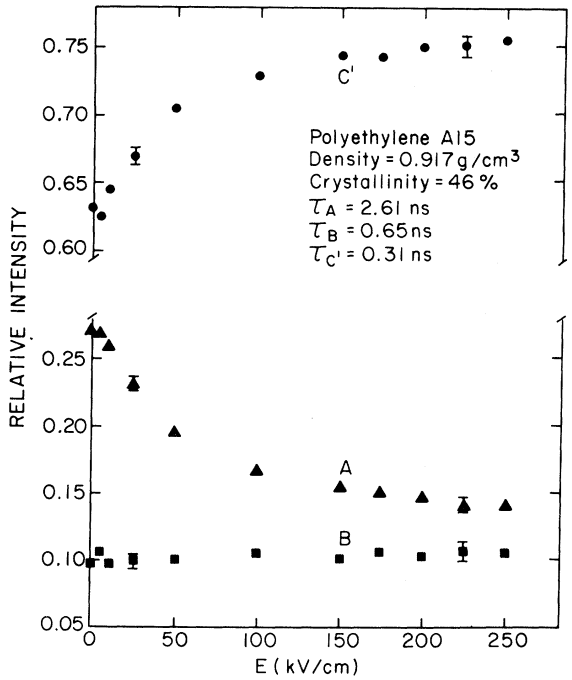

FIG. 5. Relative intensities of the three resolved components in the positron lifetime spectra of the polyethylene *A*15. Representative error bars are shown for each component.

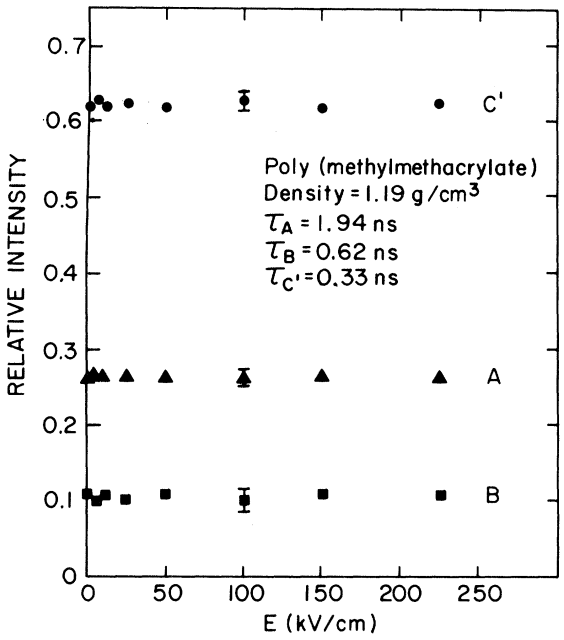

FIG. 6. Relative intensities of the three resolved components in the positron lifetime spectra for PMMA (Lucite). Representative error bars are shown.

small fields, begins to level off at field strengths above 25–50 kV/cm, and approaches a level value near 0.6 $I_A(\mathcal{E}=0)$ at the highest field strengths; $I_{C'}(\mathcal{E})$ rises at small fields and approaches a plateau concurrently with $I_A(\mathcal{E})$ at the highest applied fields; $I_B(\mathcal{E})$ stays essentially constant in the solids, and it shows a weak trend with $\mathcal{E}$ similar to that of $I_{C'}(\mathcal{E})$ in the liquids. By contrast, the intensities in the solid polymer PMMA (see Fig. 6), which contains permanent dipoles in the form of a $C=0$ group in the chain repeat unit, exhibit no field dependence whatever for applied field strengths up to 225 kV/cm.

We collate the paraffin data in a comprehensive manner by following the theoretical development presented in III. Given the measured initial slope s of the positronium yield $\Phi(\mathcal{E})$,

$$s = \left(\frac{d\Phi(\mathcal{E})}{d(\mathcal{E})}\right)_{\mathcal{E}=0}, \tag{8}$$

we define the reduced field variable

$$X(\mathcal{E}) = s\mathcal{E}. \tag{9}$$

The Ps yield data, when plotted as a function of $X(\mathcal{E})$ should yield a common curve for all homologous substances. According to III, Eq. (18), s is related to V^* as

$$s = CV^*, \tag{10}$$

where the constant C is

$$C=[e^2/2(\lambda-1)E_u\sigma_r\sigma_{sc}]^{1/2}_{CH_2}(M_{CH_2}V_0/N_L)\,, \qquad (11)$$

and depends on $\lambda\equiv\gamma_f/\gamma_r$, the ratio of the mean rate of Ps formation γ_f and the positron energy-loss rate γ_r, on E_u, the upper bound of the Ore gap, the cross sections for positron energy loss σ_r, and positron scattering σ_{sc} per CH_2 group in the medium of molecular weight $M_{CH_2}=14$ g, specific excluded volume $V_0=0.83$ cm^3/g, and $N_L=0.604\times10.$[30]

Combining Eqs. (5), (8), and (10), the initial slopes of $I_A(\mathcal{E})$ were extracted from the data and plotted in the form $s'\equiv\frac{4}{3}[dI_A(\mathcal{E})/d\mathcal{E}]_{\mathcal{E}=0}$ vs V^* in Fig. 7. The best fit to Eq. (5) (solid curve) is obtained by setting

$$X(\mathcal{E})=3.3V^*\mathcal{E}\,(\mathrm{MV/cm}). \qquad (12)$$

The data scatter by ±20% about the theoretical curve, which is comparable to the uncertainties of the points due to the differentiation of the experimental $I_A(\mathcal{E})$ data near $\mathcal{E}\to0$.

In Fig. 8 are plotted all our measured $I_A(\mathcal{E})$ data in the form

$$\Phi(\mathcal{E})=\tfrac{4}{3}I_A(\mathcal{E})\exp[V^*_{cr}/(V^*-1)],$$

Eq. (5), versus the variable $X(\mathcal{E})$, Eq. (12). The data define the locus of a common curve with a scatter comparable to the experimental uncertainties. The mean intercept $\Phi(0)$ compares well with the estimate $\Phi_0\sim6.8\ \mathrm{eV}/E_u=0.66$ based on simplest Ore gap arguments. For $X<0.1$, Φ declines linearly with X, begins to level off when $X\gtrsim0.1$, and approaches value ~0.4 when $X\gtrsim1$.

IV. DISCUSSION

The field dependence of the Ps yield in matter, $\Phi(\mathcal{E})$, reflects the balance between two opposing processes. The presence of the field enhances the escape of positrons out of the Ore gap before Ps formation: this diminishes $\Phi(\mathcal{E})$ at small fields. Mobile positrons below the Ore gap can be accelerated into the Ore gap before annihilation, where they can form Ps; this enhances $\Phi(\mathcal{E})$ at high fields. Following III, one can write

$$\Phi(\mathcal{E})=\varphi_\eta(\mathcal{E})+(1-\beta_0)[1-\varphi_\eta(\mathcal{E})]W(\mathcal{E}), \qquad (13)$$

where $\varphi_\eta(\mathcal{E})$ is the fraction of Ps formed by positrons between the upper bound E_u and the lower bound $E_l\simeq E_u-6.8$ eV of the Ore gap after their last ionizing collision. Approximately,

$$\varphi_\eta(\mathcal{E})=\Phi_0-X(\mathcal{E})\{1-\exp[(1-\eta)/X(\mathcal{E})]\}, \qquad (14)$$

where $\Phi_0\equiv\Phi(\mathcal{E}=0)\simeq1-\eta$ is the Ps yield in the absence of the field and $\eta\equiv E_l/E_u$. $W(\mathcal{E})$ denotes the probability that a positron of initial energy below the Ore gap reaches the Ore gap under the influence of the field and forms Ps. This function, derived in III, can be cast in the convenient form

$$W(\mathcal{E})=\exp[-\eta/(\lambda-1)^{1/2}X(\mathcal{E})]. \qquad (15)$$

The solid curve in Fig. 8 shows Eq. (13) for $\lambda=3$. With the value $C=3.3$ cm/MV [Eq. (12)], all data are consistent, by Eq. (11), with the mean cross section $(\sigma_r\sigma_{sc})^{1/2}_{CH_2}=(3\pm1)\times10^{-19}$ cm^2.

The assignments for the components resolved in the lifetime spectra given at the end of Sec. II imply that the annihilation rate for free thermalized positrons in the bulk is given by

$$\gamma_a=\frac{I_{C'}(\mathcal{E})\gamma_{C'}-\frac{1}{3}I_A(\mathcal{E})\gamma_{p\text{-}Ps}}{I_{C'}(\mathcal{E})-\frac{1}{3}I_A(\mathcal{E})}\,. \qquad (16)$$

We insert all our field-dependent data into Eq. (16), and find that the field-independent $\gamma_a=2.0\pm0.1$ nsec^{-1}. Setting $v_{th}\sigma_a=\gamma_a/n_{CH_2}$, where v_{th} is

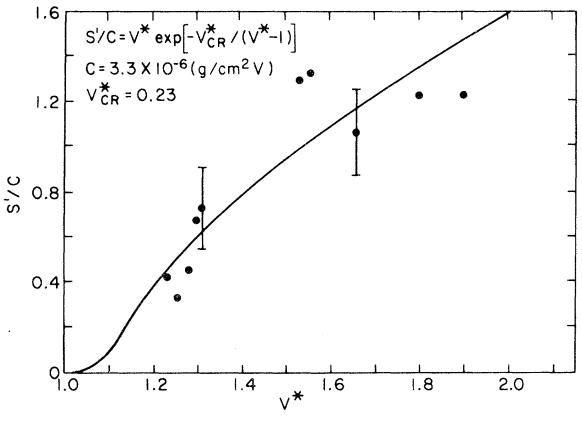

FIG. 7. Initial slope of the field-dependent Ps yield in the paraffins and polyethylenes listed in Table I plotted in dimensionless units as a function of reduced specific volume. The constant C depends on common molecular parameters as given in Eq. (11).

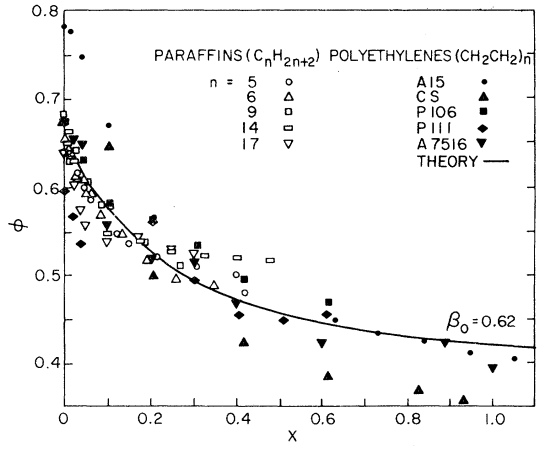

FIG. 8. Ps yield for the homologous series of paraffins and polyethylenes as a function of $\mathcal{E}$ in terms of the reduced variable $X(\mathcal{E})=CV^*\mathcal{E}$, Eq. (10).

TABLE II. Representative subexcitation parameters for the paraffins.[a]

Substance	γ_f (sec^{-1})	γ_a (sec^{-1})	γ_{sc} (sec^{-1})	γ_r (sec^{-1})	Λ	Λ_{ph}
Pentane ($n=5$)	3.5×10^{10}	1.9×10^{9}	7.8×10^{13}	1.2×10^{10}	2×10^{-4}	4.6×10^{-4}
Polyethylene ($n=\infty$)	5.0×10^{10}	3.7×10^{9}	1.1×10^{14}	1.8×10^{10}	2×10^{-4}	1.2×10^{-3}

[a]The rates are calculated for $\sigma_{sc}\equiv 2.5\times10^{-17}$ cm^2.

the thermal positron velocity, one obtains the volume rate for annihilation per CH_2 group $v_{th}\sigma_a \simeq 5\times10^{-14}$ cm^3/sec, corresponding to a cross section $(\sigma_a)_{CH_2} \simeq 7\times10^{-21}$ cm^2. For orientation, one can express σ_a in terms of the effective number of electrons per CH_2 group, N_{eff} that contribute to the annihilation of positrons,

$$v_{th}\sigma_a \simeq \pi r_e^2\, c N_{eff}\ , \tag{17}$$

where r_e is the classical electron radius and c the velocity of light. Our experimental $v_{th}\sigma_a$ value implies that $N_{eff}\simeq 6$, just the number of valence electrons per CH_2 group.

With the experimental values $\lambda=\sigma_f/\sigma_r=3$ and $(\sigma_r\sigma_{sc})^{1/2}=1\times10^{-3}\ \pi a_0^2$, we estimate the cross sections following III by setting $\sigma_r=\Lambda_{ph}\sigma_{ph}=\Lambda\sigma_{sc}$, where Λ_{ph} and Λ are the mean fractional positron energy loss per scattering collision due to phonons (cross section σ_{ph}) and to phonons and structural defects (cross section $\sigma_{sc}=\sigma_{ph}+\sigma_d$). This gives the estimates $\sigma_r=4\times10^{-21}$ cm^2, $\sigma_{sc}=2\times10^{-17}$ cm^2, and $\sigma_f=1\times10^{-20}$ cm^2 per CH_2 in condensed paraffins. The corresponding rates are listed in Table II. We estimate them to be correct within a factor of 2.

One calculates that the rate of energy loss of subexcitation positrons in a dipolar medium[31] such as PMMA is two orders of magnitude larger than the loss rate γ_r in paraffins due to positron-phonon interactions. We attribute the absence of any field dependence of the positron lifetime parameters in PMMA (Fig. 5) to this circumstance.

The root-mean-squared rest range $\langle R^2\rangle^{1/2}$ of subexcitation positrons initially of energy $E_u\sim10$ eV can be estimated from the parameters in Table II by the formula

$$\langle R^2\rangle^{1/2}=(2E_u/m\gamma_r\gamma_{sc})^{1/2}\ , \tag{18}$$

to be of the order of 10^3 Å in paraffins. Subexcitation electrons should have comparable rest ranges in such insulators. The range of subionization electrons in polyethylene has been quoted to be $\sim10^4$ Å by other evidence.[32] Through their dependence on $\gamma_r^{-1/2}$, the rest ranges in dipolar molecular insulators can be more than an order of magnitude smaller than in nonpolar substances. These quantities are of particular interest in the context of geminate ion-electron recombinations[33] and Ps formation in positron-induced spurs.[34] An extension of Eq. (15) to predict the electric breakdown strength of solids is given elsewhere.[29]

V. SUMMARY

The positron lifetime spectra in paraffins are resolved into three components with intensities I_A, I_B, $I_{C'}$, such that $I_A+I_B+I_{C'}=1$. The respective lifetimes are $\tau_A\sim3$ nsec, $\tau_B\sim0.7$ nsec, and $\tau_{C'}\sim0.3$ nsec (Table I). The density dependence of these parameters and their dependence on external electric fields is consistent with the following assignments: I_A comprises all positrons that have formed o-Ps in the substance and annihilate via electron pickoff with a lifetime τ_A; I_B comprises the fraction of positrons that have not formed Ps, but become bound in amorphous domains where they annihilate with a lifetime τ_B; $I_{C'}$ is a composite component which subsumes the p-Ps pendant of o-Ps, with lifetime $\tau_{2\gamma}=0.125$ nsec, and the fraction of free positrons that annihilate in the bulk in some 0.3 nsec. All known data appear to support these assignments.

Under the influence of a field, I_A declines toward a limiting value, while $I_{C'}$ rises and I_B remains essentially unchanged. Comprehensive curves emerge (Figs. 1, 3, and 8) which link changes of the positron lifetime spectra with changes in density, temperature, and electric field to the free volume between the molecules in these substances. The molecules are characterized by a set of cross sections per CH_2 group for the interaction with subexcitation positrons.

These cross sections should apply also to the interaction with subexcitation electrons, which governs transient electronic effects induced by ionizing radiation in insulators. One estimates subexcitation ranges for positrons and electrons of $\sim10^3$ Å in paraffins, and a diffusion constant between 0.1 and 1 cm^2/sec which should correspond to a mobility of ~10 cm^2/sec MV by Einstein's relation.

ACKNOWLEDGMENTS

We are indebted to Arthur Schwarzschild for his kind, sustained support. We benefited from discussions with Rudolf Sizmann. Gottfried Dürr assisted us in the final phases of this work, and

Shirley McArthur helped in the preparation of the manuscript.

APPENDIX A: NARROW ANGULAR CORRELATION COMPONENT

As shown in I and V, the function $\xi(S, V^*)$ in Eq. (2) is related to the zero-point energy E_0 as the lowest eigenvalue of the Schrödinger equation for the Ps wave function. We introduce[35] $\eta_0(S, V^*) \equiv [1 - \xi^2(S, V^*)/S]^{1/2}$, and write

$$E_0(S, V^*) = (\hbar^2 S/4mr_0^2)\eta_0^2(S, V^*). \quad \text{(A1)}$$

The width Γ_N of the commonly observed narrow component in the angular correlation between the two annihilation gamma rays in Ps-forming substances is attributed to the root-mean-squared zero-point Ps momentum, $\langle p^2\rangle^{1/2} = (E_0/4m)^{1/2}$, carried away in p-Ps annihilation. The Fourier transforms of the Ps wave functions derived in I and V, when squared, give the momentum distributions, $F(p)dp$, of the emerging γ's in the narrow component. They have the approximate form $F(p)dp = [4\langle p^2\rangle/\pi(p^2 + \langle p^2\rangle)^2]dp$. Experimentally, one measures the momentum at one-half the maximum of the narrow distribution, $p_{1/2}$. It is related to $\langle p^2\rangle$ as $p_{1/2} \simeq [(\sqrt{2} - 1)\langle p^2\rangle]^{1/2}$. Since $\Gamma_N = 2p_{1/2}/m_+c$ rad, where c is the velocity of light, we obtain with Eq. (A1)

$$\Gamma_N(\text{mrad}) \simeq [2.5 g_\mu^{1/2} S^{1/2}/r_0\ (\text{Å})]\eta_0(S, V^*), \quad \text{(A2)}$$

if Γ_N is given in mrad, and r_0 in Å. The geometrical factor g_u depends on the experiment. In long-slit geometries, one measures the momentum distribution in some z direction p_z. The factor g_μ accounts for this projection by taking the average o overall orientations, θ, of the lattice geometry relative to the z axis as appropriate for polycrystalline or disordered materials,

$$g_\mu = \begin{cases} \langle \cos^2\theta\rangle \mu = 1/2\mu & \text{for } \mu = 1, 2 \\ 1/\mu & \text{for } \mu = 3\ . \end{cases} \quad \text{(A3)}$$

It was pointed out in V that, to a good approximation, one can set $\eta_0 = [1 + F(S, V^*)]^{-1/3}$ and, at temperatures $T^* < T_M^*$, one has $\eta_0 \simeq (\tau_0/\tau_P)^{1/3}$. Equation (A2) becomes

$$\Gamma_N(\text{mrad}) \simeq [2.5 g_\mu^{1/2} S^{1/2}/r_0\ (\text{Å})](\tau_0/\tau_P)^{1/3}, \quad \text{(A4)}$$

which interlinks Γ_N and $\tau_A \simeq \tau_P$. The parameter S can be determined from variations of τ_A with temperature or estimated by Eq. (A4) from experimental values of Γ_N and τ_A. The radius r_0 may be related to the excluded volume as $V_0^{1/\mu}$, where $\mu = 1$, 2, 3 for conditions of planar, cylindrical and spherical molecular geometry, respectively, and can be estimated by setting $r_0 \simeq \sigma/2$, where σ is the Lennard-Jones molecular diameter.[36]

We emphasize that despite the complexities of the detailed molecular potential encountered by Ps atoms in condensed matter, it suffices to characterize the potential only by one parameter S. Electron pickoff occurs when Ps is in the lattice ground-state with wave vector $\vec{k}_{Ps} \simeq 0$, and S-wave scattering predominates. Although cast in the terms of a model with square potentials, this should not be viewed as a basic limitation of Eq. (1). In fact, the S dependence of the theory contains all the information that can be extracted from these experiments about the real potential which determines the wave function overlap leading to electron pickoff.

For the paraffins, $g_\mu = \frac{1}{4}$ and $S \simeq 60$. This yields, by Eq. (A2), $\Gamma_N \simeq 3.5$ mrad, in agreement with the value measured by Patterson and Stewart.[37]

It follows from Eq. (A4) that when τ_P decreases, e.g., because of the cooling of a substance, the narrow component widens. This circumstance can make it difficult to resolve the fraction of annihilations occuring in the narrow component [~ (3–10)%] and may lead to estimates of the narrow component that are too low if compared to $I_A/3$.[38]

APPENDIX B: A^+ CENTERS IN PARAFFINS

The intermediate lifetime component I_B is unaffected by the electric field and attributed to positrons forming A^+ centers in the disordered domains of the paraffins. One estimates a lower limit for the A^+ center dissociation energy by noting that in a field $\mathcal{E}$ the energy, E_λ, for positron escape from the A_+ center[39] is reduced by $-e\mathcal{E}r_T\cos\theta$, where r_T is the effective trap radius and $z = r\cos\theta$ the coordinate from the origin in the A^+ center along the field direction. Given the attempt frequency per unit solid angle, $\nu_{ph}/4\pi$, the escape rate λ becomes

$$\begin{aligned}\lambda(\mathcal{E}) &= \frac{\nu_{ph}}{4\pi}\int_0^{2\pi} d\varphi \int_0^{\pi} d\theta \sin\theta \\ &\quad \times \exp[(-E_\lambda - e\mathcal{E}r_T\cos\theta)/k_BT] \quad \text{(B1)} \\ &= \nu_{ph}\exp(-E_\lambda/k_BT)(k_BT/e\mathcal{E}r_T) \\ &\quad \times \sinh(e\mathcal{E}r_T/k_BT),\end{aligned}$$

where $\nu_{ph} \simeq k_BT/h$ is of the order of 1 psec^{-1}. The field independence of I_B implies that $\lambda(\mathcal{E})\tau_B < 1$ in our range of field strengths, which obtains for $E_\lambda > 0.23$ eV. This value is comparable to the affinity of a positron to a paraffin molecule.

*Work supported in part by the United States Defense Atomic Support Agency and the National Science Foundation.

†Present address: Intelcom Rad Tech, San Diego, Calif. 92138.

[1]W. Brandt, S. Berko, and W. W. Walker, Phys. Rev. 120, 1289 (1960); 121, 1864E (1961) (I).

[2]W. Brandt and I. Spirn, Phys. Rev. 142, 231 (1966) (II).

[3]W. Brandt and H. Feibus, Phys. Rev. 174, 454 (1968) (III); 184, 277 (1969) (IV).

[4]W. Brandt and J. H. Fahs, Phys. Rev. B 2, 1425 (1970); B 3, 2370E (1971) (V).

[5]W. Brandt, in *Positron Annihilation*, edited by A. T. Stewart and L. O. Roellig (Academic, New York, 1967), p. 155ff.

[6]M. Deutsch and C. S. Brown, Phys. Rev. 85, 1047 (1952).

[7]S. Marder, V. W. Hughes, C. S. Wu, and W. Bennett, Phys. Rev. 103, 1258 (1956).

[8]F. E. Obenshain and L. A. Page, Phys. Rev. 125, 573 (1961).

[9]G. E. Manuzio and C. Rizzuto, Nuovo Cimento B 43, 166 (1966).

[10]A. Bisi, F. Bisi, L. Fasana, and L. Zappa, Phys. Rev. 122, 1709 (1961).

[11]W. Brandt and J. Wilkenfeld, Bull. Am. Phys. Soc. 14, 523 (1969)]; J. Wilkenfeld, Thesis, 1973 (unpublished).

[12]R. W. Crowe, A. H. Sharbaugh, and J. K. Bragg, J. Appl. Phys. 25, 1480 (1954).

[13]K. Takayanagi and M. Inokuti, J. Phys. Soc. Jpn. 23, 1412 (1967).

[14]G. Present, A. Schwarzschild, I. Sprin, and N. Wotherspoon, Nucl. Instrum. Methods 31, 71 (1964).

[15]The authors wish to thank T. Karcher for this calculation.

[16]J. R. Stevens and P. C. Lichtenberger, Phys. Rev. Lett. 29, 166 (1972).

[17]J. B. Cumming, Brookhaven National Laboratory Report No. 6470, 1962 (unpublished).

[18]W. Davidson, Argonne National Laboratory Report, 1966 (unpublished).

[19]The authors wish to thank Dr. J. M. Watkins, Jr., of the Plastics Department of E. I. DuPont de Nemours Co. for providing us with the polyethylene, Teflon, and FEP samples, and their characterization in terms of density and fractional volume crystallinity.

[20]American Petroleum Institute, Research Project 44: *Selected Values of the Properties of Hydrocarbons and Related Compounds* (Chemical Thermodynamics Center, Texas A & M University), published as a series of data sheets.

[21]I. Adamczewski, *Ionization, Conductivity, and Breakdown in Dielectric Liquids* (Taylor and Francis, London, 1969), p. 369.

[22]S. J. Tao and J. Green, Proc. Phys. Soc. Lond. 85, 463 (1965).

[23]R. K. Wilson, P. O. Johnson, and R. Stump, Phys. Rev. 129, 2091 (1963).

[24]P. R. Gray, C. F. Cook, and G. P. Sturm, Jr., J. Chem. Phys. 48, 1145 (1968).

[25]A. P. Buchikhin, V. I. Goldanskii and V. P. Shantarovich, Zh. Exp. Theor. Fiz. Pis'ma Red. 13, 624 (1961) [JETP Lett. 13, 444 (1971)].

[26]B. V. Thosar, V. G. Kulkarni, R. G. Lagu, and G. Chandra, Phys. Lett. A 33, 125 (1970).

[27]W. DeSorbo, J. Chem. Phys. 21, 1144 (1953).

[28]These assignments are consistent with the combined lifetime and angular correlation coincidence measurements on Teflon made by J. D. McGervey and V. F. Walters [Phys. Rev. B 2, 2421 (1970)].

[29]W. Brandt, in *Proceedings of the Third International Conference on Positron Annihilation*, 1973, Otaniemi, Finland (Springer, Berlin, 1975); Appl. Phys. 5, 1 (1974).

[30]In the related expression in the text following Eq. (18) in III, the factor $\sqrt{\frac{3}{2}}$ should read $\sqrt{\frac{2}{3}}$.

[31]H. Fröhlich and R. L. Platzman, Phys. Rev. 92, 1152 (1953).

[32]J. F. Fowler, Proc. R. Soc. A 236, 464 (1956).

[33]W. Brandt and R. H. Ritchie, *Physical Mechanisms in Radiation Biology* (U.S. AEC Publication CONF-721001, 1974), pp. 20–46.

[34]O. E. Mogensen, J. Chem. Phys. 60, 998 (1974).

[35]In paper V, $\eta_0 S^{1/2}$ is denoted by η.

[36]W. Brandt, J. Chem. Phys. 24, 501 (1956); 26, 262 (1957).

[37]T. M. Patterson and A. T. Stewart, in Ref. 5.

[38]G. De Blonde, S. Y. Chuang, B. G. Hogg, D. P. Kerr, and D. M. Miller, Can. J. Phys. 50, 1619 (1972). It is reported here that no narrow component could be isolated in the angular-correlation spectrum of hydrocarbons below the melting point despite the fact that the longest lived of the two resolved lifetime components observed in the liquid persists. This may be caused, in part, by the merging of two components, corresponding to our I_A and I_B, into one, of which only a fraction is then indicative of Ps formation, and, in part, by the widening of Γ_N on freezing.

[39]W. Brandt and L. J. Cheng, Phys. Lett. A 50, 439 (1975).